Frost, Ray L. and Keeffe, Eloise C. and Cejka, Jiri and Sejkora, Jiri (2009) *Raman spectroscopic study of the uranyl mineral metauranospinite Ca[(UO2)(AsO4)]2.8H2O.* Journal of Raman Spectroscopy, 40(12). pp. 1786-1790.

Raman spectroscopic study of the uranyl mineral metauranospinite $Ca[(UO_2)(AsO_4)]_2 \cdot 8H_2O$

Jiří Čejka, [1,2] Jiří Sejkora, [1] Ray L. Frost, [2] • Eloise C. Keeffe [2]

[1] National Museum, Václavské náměstí 68, CZ-115 79 Praha 1, Czech Republic.

[2] Inorganic Materials Research Program, School of Physical and Chemical Sciences, Queensland University of Technology, GPO Box 2434, Brisbane Queensland 4001, Australia.

Abstract

Raman spectra of metauranospinite $Ca[(UO_2)(AsO_4)]_2 \cdot 8H_2O$ complemented with infrared spectra were studied. Observed bands were assigned to the stretching and bending vibrations of $(UO_2)^{2+}$ and $(AsO_4)^{3-}$ units and of water molecules. U-O bond lengths in uranyl and O-H…O hydrogen bond lengths were calculated from the Raman and infrared spectra.

Keywords: metauranospinite, mineral, uranyl, arsenate, molecular water, Raman, infrared, spectroscopy

Introduction

According to Finch and Murakami [1], uranyl phosphates and uranyl arsenates constitute by far the most structurally diverse group of uranyl minerals. Uranyl arsenates precipitate where dissolved $(AsO_4)^{3-}$ ions are available, which is most commonly where arsenide minerals and As-bearing sulfide minerals are being oxidized. This is, why uranyl arsenates commonly occur in the same localities as uranyl sulfates [1].

Orthoarsenates of hexavalent uranium may be divided into three general classes based on the polymerization of polyhedra of higher bond-valence: chain, sheet, and framework structure [2,3]. The layered structures of the uranyl orthophosphates and orthoarsenates are

• Author to whom correspondence should be addressed (r.frost@qut.edu.au)

dominated by the autunite-type sheet with general stoichiometry $M^{n+}[(UO_2)(XO_2)]_n \cdot mH_2O$, where M = monovalent, divalent or trivalent cations, and X = P or As. The corrugated autunite-type sheet consists of uranyl square dipyramids that share their equatorial vertices with phosphate or arsenate tetrahedra to form a checkerboard-like pattern. The interlayer contains water molecules and either monovalent-, divalent-, or trivalent cations. The sheets are linked by hydrogen bonds, and to a lesser extent also through bonds from the interlayer cations to oxygens of the sheet [3]. Locock [3] assumes that uranospinite is isostructural with autunite, $Ca[(UO_2)(PO_4)]_2 \cdot 11H_2O$, synthetic $Sr[(UO_2)(PO_4)]_2 \cdot 11H_2O$ and $Sr[(UO_2)(AsO_4)]_2 \cdot 11H_2O$, and has therefore the formula $Ca[(UO_2)(AsO_4)]_2 \cdot 11H_2O$. According to Anthony et al. [4] and Mandarino and Back [5], uranospinite may contain 10 H_2O pfu. However, these authors do not give any chemical analysis of metauranospinite. On studying synthetic phases in the system $Ca[(UO_2)(AsO_4)]_2 – H_2O$, Mrose [6] described an octahydrate, Leonova [7] dodeca-, deca-, octa- and hexahydrates. Walenta [8-10] assumes that natural and synthetic uranospinite and metauranospinite contain 10 and 6 water molecules pfu, respectively. Hoffmann and Weigel [11-13] studied dehydration of synthetic uranospinite under constant water partial pressure and observed hydrates with 10, 8, 6, 3-4 H_2O pfu and the anhydrous compound, however, water content determinations suggested also hydrates with 8, 9 and 12 H_2O. Ambartsumyan [14] studied thermal decomposition of a minerals phase indicated as uranospinite containing 8 H_2O pfu. Chernorukov et al. [15] presented synthesis, X-ray powder patterns, thermal analysis and infrared spectra of $Ca[(UO_2)(AsO_4)]_2 \cdot xH_2O$, where x = 12, 6, 3. Mandarino and Back [5] assume that metauranospinite contains 8 H_2O pfu. Similar data are given by Anthony et al. [4]. Locock [2,3] writes in both review papers that metauranospinite may contain 6.5 H_2O, however, this is not given with any certainty. Uranospinite easily dehydrates to metauranospinite and metauranospinite may rehydrate to uranospinite.

Metauranospinite, $Ca[(UO_2)(AsO_4)]_2 \cdot 8H_2O$, is probably tetragonal, with unit cell parameters a = 7.14, c = 17.00, Z=2, space group is not known [4]. However, because of some discrepancies in optical properties in the autunite-metautunite mineral group – none of the fully hydrated minerals have tetragonal symmetry, although pseudosymmetry is common [3], metauranospinite is biaxial negative, its symmetry may be therefore lower and only pseudotetragonal. No X-ray single crystal structure data for metauranospinite are as yet available. Neither uranospinite nor metauranospinite have been therefore included in the

structural hierarchy of crystal structures of uranyl compounds and minerals established by Burns [16]

Some information concerning the infrared spectrum of metauranospinite may be inferred from the paper by Chernorukov et al. [15], who published several synthetic phases in the system $Ca[(UO_2)(AsO_4)]_2 - H_2O$, however, without any detailed interpretation of their infrared spectra.

This paper is a part of the series of the vibrational spectroscopy studies of secondary minerals formed in the oxidation zone and related compounds inclusive uranyl minerals.

Experimental

Mineral

The studied sample of the mineral metauranospinite was found at the mine dump 16 (Příbram - Háje), the Příbram uranium-polymetallic ore district, central Bohemia, Czech Republic [17], and is deposited in the mineralogical collections of the National Museum Prague. The sample was analyzed for phase purity by X-ray powder diffraction. No minor significant impurities were found. Its refined tetragonal unit-cell parameters, *a* 7.161(3), *c* 17.15(2) Å, *V* 880(1) $Å^3$, are comparable with the data published for this mineral phase [4]. The mineral was analysed by electron microprobe (Cameca SX100, WD mode) for chemical composition. The results (mean of 7 point analyses) are Na_2O 0.03, CaO 4.45, FeO 0.15 MgO 0.78, As_2O_5 23.82, P_2O_5 0.02, UO_3 59.00, H_2O 14.80 wt. %, sum 103.04 wt. %. The water content was inferred from the thermal analysis of metauranospinite sample. The resulting empirical formula on the basis of (As+Si+P+V) = 2 apfu is $(Ca_{0.76}Mg_{0.19}Fe_{0.02}Na_{0.01})_{\Sigma 0.98}(UO_2)_{1.99}(AsO_4)_{2.00}.7.92H_2O$.

Raman spectroscopy

The crystals of metauranospinite were placed and oriented on the stage of an Olympus BHSM microscope, equipped with 10x and 50x objectives and part of a Renishaw 1000 Raman microscope system, which also includes a monochromator, a filter system and a Charge Coupled Device (CCD). Further details have been published [18-26].

Raman spectra of metauranospinite are given in Figs. 1-4.

IR spectroscopy

Infrared spectra were obtained using a Nicolet Nexus 870 FTIR spectrometer with a smart endurance single bounce diamond ATR cell. Spectra over the 4000–525 cm^{-1} range were obtained by the co-addition of 64 scans with a resolution of 4 cm^{-1} and a mirror velocity of 0.6329 cm/s. Spectra were co-added to improve the signal to noise ratio. These spectra are fundamentally reflectance spectra and are transformed to absorbance type spectra.

Spectral manipulation such as baseline adjustment, smoothing and normalisation were performed using the Spectracalc software package GRAMS (Galactic Industries Corporation, NH, USA). Band component analysis was undertaken using the Jandel 'Peakfit' software package which enabled the type of fitting function to be selected and allows specific parameters to be fixed or varied accordingly. Band fitting was done using a Lorentz-Gauss cross-product function with the minimum number of component bands used for the fitting process. The Gauss-Lorentz ratio was maintained at values greater than 0.7 and fitting was undertaken until reproducible results were obtained with squared correlations of r^2 greater than 0.995.

Infrared spectra of metauranospinite are provided in the supplementary information Figs. S1 – S3.

Results and discussion

Raman and infrared spectroscopy

A free uranyl, $(UO_2)^{2+}$, point symmetry $D_{\infty h}$, should exhibit three fundamental modes: the Raman active symmetric stretching vibration ν_1 (~900-750 cm^{-1}), the infrared active bending vibration ν_2 (δ) (~300-200 cm^{-1}), and the infrared active antisymmetric stretching vibration ν_3 (~1000-850 cm^{-1}). The bending mode is doubly degenerate since it occurs in two mutually perpendicular planes. It can split into its two components when the uranyl ion is placed in an external force field. Thus, the linear uranyl group, point symmetry $D_{\infty h}$, has four normal vibrations, but only three fundamentals. The Raman active ν_1 $(UO_2)^{2+}$ appears in the infrared spectrum only in the case of substantial symmetry lowering. A lowering of symmetry ($D_{\infty h} \Rightarrow C_{\infty v}$, C_{2v} or C_s causes both the activation of all three fundamentals in the infrared and Raman spectra and the activation of their overtones and combination vibrations [27].
The doubly degenerate ν_2 (δ) $(UO_2)^{2+}$ bending vibration is infrared active, and a decrease of symmetry can cause splitting of this vibration into two infrared and Raman active components. Coincidences between uranyl bending vibrations and U-O_{ligand} vibrations were observed in some uranyl synthetic compounds and minerals [27].

Arsenate ion, $(AsO_4)^{3-}$, is a tetrahedral unit with Td symmetry and exhibit four fundamental vibrations: the symmetric stretching vibration ν_1 (A_1) (818 cm^{-1}), the doubly degenerate bending vibration ν_2 (E) (350 cm^{-1}), the triply degenerate antisymmetric stretching vibration ν_3 (F_2) (786 cm^{-1}), and the triply degenerate bending vibration ν_4 (F_2) (398 cm^{-1}) [28-32]. The F_2 modes are Raman and infrared active, whereas A1 and E modes are Raman active only. According to Frost et al. [24], the ν_1 $(AsO_4)^{3-}$ vibration may coincide with the ν_3 $(AsO_4)^{3-}$ vibration. It should be noted that the wavenumber of the ν_1 $(AsO_4)^{3-}$ may be greater than that of the ν_3 $(AsO_4)^{3-}$ which is an inversion of the normal behavior shown by most tetrahedral ions, although such an inversion is not unique [33,34].

According to Myneni et al. [31], the Td symmetry of $(AsO_4)^{3-}$ unit is rarely preserved in minerals and synthetic compounds, because of its strong affinity to protonate, hydrate, and complex with metal ions. Such chemical interactions reduce $(AsO_4)^{3-}$ tetrahedral symmetry to

either C_{3v}/C_3 (corner sharing), C_{2v}/C_2 (edge-sharing, bidentate binuclear), or C_1/C_s (corner sharing, edge-sharing, bidentate binuclear, multidentate]. This symmetry lowering is connected with activation of all vibrations in infrared and Raman spectra and splitting of doubly and triply degenerate vibrations. Nine normal modes may be Raman and infrared active in the case of the lowest C_s symmetry [35].

U-O vibrations in uranyl coordination polyhedra

The Raman spectrum of metauranospinite in the 600 to 1200 cm^{-1} is displayed in Fig.1. In the region 880-950 cm^{-1} two Raman bands at 907 and 896 cm^{-1}. These bands are attributed to the ν_3 $(UO_2)^{2+}$ antisymmetric stretching vibration. Three infrared bands at 951, 934 and 888 cm^{-1} may be also assigned to this vibration (600-1000 cm^{-1}; Fig. 1S). Raman and infrared bands in natrouranospinite attributed to the ν_3 $(UO_2)^{2+}$ were observed at 904 and 893 cm^{-1}, and 950, 940 and 901 cm^{-1}, respectively. There are two empirical relations by Bartlett and Cooney [36], $R_{U-O} = 91.41\nu_3^{-2/3} + 0.804$ Å and $R_{U-O} = 106.5\nu_1^{-2/3} + 0.565$ Å, which enable to infer U-O bond lengths in uranyl from observed wavenumbers of the ν_3 and ν_1 $(UO_2)^{2+}$ vibrations, respectively. Calculated U-O bond lengths are (Å/cm^{-1}) 1.780/907, 1.788/896 (Raman) and 1.749/951, 1.761/934, 1.793/888 (infrared). These values are close to those for synthetic and natural uranyl compounds possessing the same uranyl anion sheet topology as expected in the crystal structure of metauranospinite [16].

There may be expected some coincidences of the ν_3 and ν_1 $(UO_2)^{2+}$ stretching vibrations and the ν_3 and ν_1 $(AsO_4)^{3-}$ stretching vibrations. In infrared spectra of synthetic phases in the system $Ca[(UO_2)(AsO_4)]_2.x\ H_2O$ (x = 12, 6, 3), Chernorukov et al. [15] assigned bands in the region of 900 cm^{-1} to the stretching vibrations of the uranyl units, while those close to 820 and 450 cm^{-1} to the stretching and bending vibrations of the arsenate units, respectively without any more detailed interpretation. The Raman spectrum of metauranospinite in the 100 to 500 region is shown in Fig. 2. A band at 275 cm^{-1} is connected with the ν_2 (δ) $(UO_2)^{2+}$ bending vibrations. Bands with lower wavenumbers may be related to the lattice vibrations. In the region 800 to 850 cm^{-1}, there are observed two Raman bands (815 and 806 cm^{-1} / a shoulder) and one infrared band at 804 cm^{-1}, which may be assigned to the ν_1 $(UO_2)^{2+}$ symmetric stretching vibrations, however, a coincidence with the ν_3 $(AsO_4)^{3-}$ antisymmetric stretching vibrations and/or the ν_1 $(AsO_4)^{3-}$ symmetric stretching vibrations. This may be supported by relatively strong intensity of the infrared band at 804 cm^{-1} in comparison with

194 the low intensity of infrared bands at 888, 934 and 951 cm^{-1}. Calculated U-O bond lengths in
195 uranyl are (Å/cm^{-1}) 1.796/815 and 1.806/806 (Raman) and 1.807/804 (infrared). These values
196 are comparable with those calculated with the wavenumbers of the ν_3 $(UO_2)^{2+}$ (see above)
197 and inferred U-O bond lengths for synthetic and natural uranyl compounds having the same
198 or similar uranyl anion sheet topology [16].
199
200 ***$(AsO_4)^{3-}$ tetrahedra vibrations***
201
202 Raman bands at 907, 896, 815 and 806 cm^{-1} and infrared bands at 888, 804 and 744
203 cm^{-1} are located in the region of the $(AsO_4)^{3-}$ stretching vibrations and some of them may be
204 therefore in fact connected with the ν_1 $(AsO_4)^{3-}$ symmetric stretching vibrations and the split
205 triply degenerate ν_3 $(AsO_4)^{3-}$ antisymmetric stretching vibrations. However, as mentioned in
206 the preceding paragraph, e.g. the Raman bands at 907 and 896 cm^{-1} may be assigned to the ν_3
207 $(UO_2)^{2+}$ antisymmetric stretching vibrations and the Raman bands at 815 and 806 cm^{-1} and
208 the infrared band at 804 cm^{-1} to the ν_1 $(UO_2)^{2+}$ symmetric stretching vibrations. The Raman
209 spectrum of metauranospinite in the 600 to 1200 cm^{-1} region is displayed in Fig. 1, and the
210 infrared spectrum of metauranospinite in the 600 to 1000 cm^{-1} in Fig.1S.
211
212 Because of the coincidence mentioned above, a more detailed tentative assigment
213 makes problems and may be qualified as very speculative. According to Nakamoto [37],
214 wavenumbers of fundamental vibrations of the $(AsO_4)^{3-}$ tetrahedra are ν_1 837 cm^{-1}, ν_2 349
215 cm^{-1}, ν_3 878 cm^{-1}, ν_4 463 cm^{-1}, but it was sometimes observed that the wavenumber of the ν_1
216 $(AsO_4)^{3-}$ may be greater that that of the ν_3 $(AsO_4)^{3-}$. The T_d symmetry lowering causes that
217 the triply degenerate antisymmetric vibration ν_3 $(AsO_4)^{3-}$ and the triply degenerate bending
218 vibration ν_4 $(AsO_4)^{3-}$ may split. In such cases the ν_1 and ν_3 $(AsO_4)^{3-}$ vibrations may coincide.
219 The Raman spectrum of metauranospinite in the 100 to 500 cm^{-1} region is displayed in Fig. 2.
220 Raman bands at 458 and 397 cm^{-1} were attributed to the triply degenerate ν_4 $(AsO_4)^{3-}$ bending
221 vibrations, and a Raman band at 322 cm^{-1} to the doubly degenerate ν_2 $(AsO_4)^{3-}$ bending
222 vibration. Some coincidence of these bands with libration modes of water molecules and/or ν
223 U-O_{ligand} stretching vibrations cannot be excluded.
224
225 ***OH stretching and bending vibrations of water molecules***
226

The Raman spectrum of metauranospinite in the 3000 to 3800 cm^{-1} region is displayed in Fig. 3. The infrared spectrum of metauranospinite in the 2600 to 3800 cm^{-1} region is given in Fig. 2S. Raman bands at 3549, 3428 and 3238 cm^{-1} and infrared bands at 3600, 3414, 3208 and 2926 cm^{-1} are assigned to the ν OH stretching vibrations of water molecules and are connected to the O-H…O hydrogen bonds formed in the crystal structure of metauranospinite (Å/cm^{-1}) ~3.0/3549, 2.83/3428 and 2.72/3238 (Raman), >3.2/3600, 2.81/3414, 2.71/3208 and 2.64/2926 (infrared) [40]. Observed infrared spectrum is comparable with that of natrouranospinite [35, 39] .

Raman bands (Fig. 4) at 1366, 1518, 1787, 1891 and 2106 cm^{-1} and infrared bands (Fig. 3S) at 1080, 1114, 1137, 1168, 1391, 1430, 1471 and 1571 cm^{-1} are probably connected with some overtones and combination bands. Neither detectable impurities or practically nor especially isomorphic P ⇔ As substitutions may be expected in the metauranospinite sample studied.

The Raman band at 1617 cm^{-1} and the infrared band at 1637 cm^{-1} are attributed to the ν_2 (δ) H_2O bending vibrations.

Conclusions

(a) Raman and infrared spectrum of metauranospinite from Příbram - Háje, Czech Republic were measured.

(b) The spectra of metauranospinite were tentatively interpreted and observed bands were assigned to the stretching and bending vibrations of $(UO_2)^{2+}$and $(AsO_4)^{3-}$ ions and water molecules.

(c) U-O bond lengths in uranyl, $(UO_2)^{2+}$, were calculated from observed wavenumber of the uranyl stretching vibrations with two empirical relations by Bartlett and Cooney [36] and compared with U-O bond lengths of natural and synthetic compounds possessing the same uranyl anion sheet topology [16].

(d) O-H…O hydrogen bonds were calculated with the empirical data by Libowitzky [40].

Acknowledgments

This work was financially supported by Ministry of Culture of the Czech Republic (MK00002327201) to Jiří Sejkora. The financial and infra-structure support of the Queensland University of Technology, Inorganic Materials Research Program is gratefully acknowledged. The Australian Research Council (ARC) is thanked for funding the instrumentation.

References

1. Finch RJ, Murakami T *Reviews in Mineralogy* **1999**, *38*, 91-179.
2. A.J. Locock, In Structural chemistry of inorganic actinide compounds, (S.V. Krivovichev, P.C. Burns, I.G. Tananaev, Eds.), p. 217-278, Elsevier Amsterdam 2007.
3. Locock AJ *Proc. Russ. Mineral. Soc.* **2007**, *136*, 115-137.
4. Anthony JW, Bideaux RA, Bladh KW, Nichols MC *Handbook of Mineralogy*; Vol IV Mineral Data Publishing: Tuscon, Arizona, USA, 2000; Vol. 4.
5. Mandarino JA, Back ME *Fleischer's glossary of mineral species* The Mineralogical Record Inc.: Tucson , Arizona, 2004.
6. Mrose ME *American Mineralogist* **1953**, *38*, 1159-1168.
7. Leonova EN *Trudy Instituta geologii rudnykh mestorozhdenii, petrographii, mineralogii i geokhimii AN SSSR (in Russian).* **1958**, *30*, 37-55.
8. Walenta K *Jahreshefte des Geologischen. Landesamts Baden-Württemberg* **1958**, *3*, 17-51.
9. Walenta K *Tschermaks Mineralogische und Petrographische Mitteilungen* **1965**, *9*, 252-282.
10. Walenta K *Chemie der Erde* **1965**, *24*, 254-278.
11. Hoffmann G, Thesis, Ludwig-Maxmilian University, Munich, 1972.
12. Weigel F, Hoffmann G *Journal of the Less-Common Metals* **1976**, *44*, 99-123.
13. F. Weigel In Handbook of physics and chemistry of actinides, (A.J. Freeman, C. Keller, Ed.), p. 243-288, Elsevier Amsterdam 1985.
14. Ambartsumyan TL, Basalova GI, Gorzhevskaya SA, Nazarenko NG, R. P. Khodzhaeva *Thermal investigations of uranium and uranium-bearing minerals. Gosatomizdat Moscow* **1961 (in Russian).**
15. Chernorukov NG, Karyakin NV, Suleimanov EV, Belova YS *Zhurnal Neorganicheskoy Khimii* **1996**, *41*, 39-42.
16. Burns PC *Canadian Mineralogist* **2005**, *43*, 1839-1894.
17. J. Sejkora, J. Cejka, A. Gabasova, J. Jindra, Bulletin mineralogicko-petrologického Oddělení Národního Muzea (Praha) 10 (2002) 273-278 (in Czech).
18. Frost RL, Cejka J, Ayoko G *Journal of Raman Spectroscopy* **2008**, *39*, 495-502.
19. Frost RL, Cejka J, Ayoko GA, Dickfos MJ *Journal of Raman Spectroscopy* **2008**, *39*, 374-379.

20. Frost RL, Cejka J, Dickfos MJ *Journal of Raman Spectroscopy* **2008**, *39*, 779-785.
21. Frost RL, Dickfos MJ, Cejka J *Journal of Raman Spectroscopy* **2008**, *39*, 582-586.
22. Frost RL, Hales MC, Wain DL *Journal of Raman Spectroscopy* **2008**, *39*, 108-114.
23. Frost RL, Keeffe EC *Journal of Raman Spectroscopy* **2008**, *in press*.
24. Frost RL, Locke A, Martens WN *Journal of Raman Spectroscopy* **2008**, *39*, 901-908.
25. Frost RL, Reddy BJ, Dickfos MJ *Journal of Raman Spectroscopy* **2008**, *39*, 909-913.
26. Palmer SJ, Frost RL, Ayoko G, Nguyen T *Journal of Raman Spectroscopy* **2008**, *39*, 395-401.
27. Cejka J *Reviews in Mineralogy* **1999**, *38*, 521-622.
28. Frost RL, Cejka J, Weier ML, Martens WN, Ayoko GA *Journal of Raman Spectroscopy* **2007**, *38*, 398-409.
29. Frost RL, Weier ML, Ayoko GA, Martens W, Cejka J *Mineralogical Magazine* **2006**, *70*, 299-307.
30. Frost RL, Carmody O, Erickson KL, Weier ML, Henry DO, Cejka J *Journal of Molecular Structure* **2004**, *733*, 203-210.
31. Myneni SCB, Traina SJ, Waychunas GA, Logan TJ *Geochim. Cosmochim. Acta* **1998**, *62*, 3285-3300.
32. Myneni SCB, Traina SJ, Waychunas GA, Logan TJ *Geochim. Cosmochim. Acta* **1998**, *62*, 3499-3514
33. Vansant FK, Veken BJVd, Desseyn HO *J. Mol. Struct.* **1973**, *15*, 425-437.
34. Busey RH, Keller OL *J. Chem. Phys.* **1964**, *41*, 215-225.
35. Ross SD In *The infrared spectra of minerals* Farmer VC, Ed.; Mineralogical Society: London 1974.
36. Bartlett JR, Cooney RP *J. Mol. Struct.* **1989**, *193*, 295-300.
37. K. Nakamoto, Infrared and Raman spectra of inorganic and coordination compounds, Wiley New York 1986.

335 ***List of Figures***

336

350

351

352

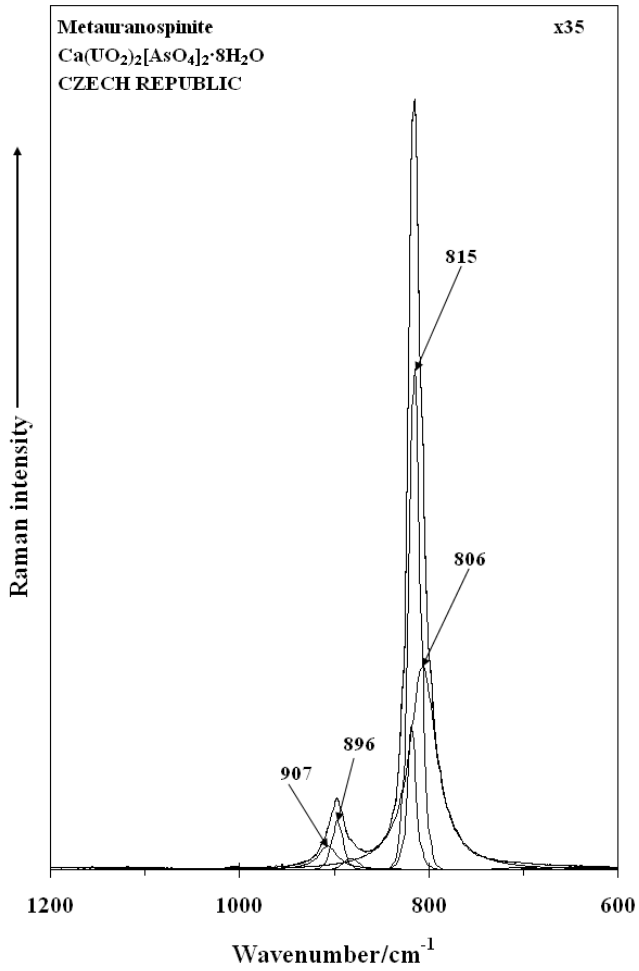

353

354

355

356 **Figure 1**

357

358

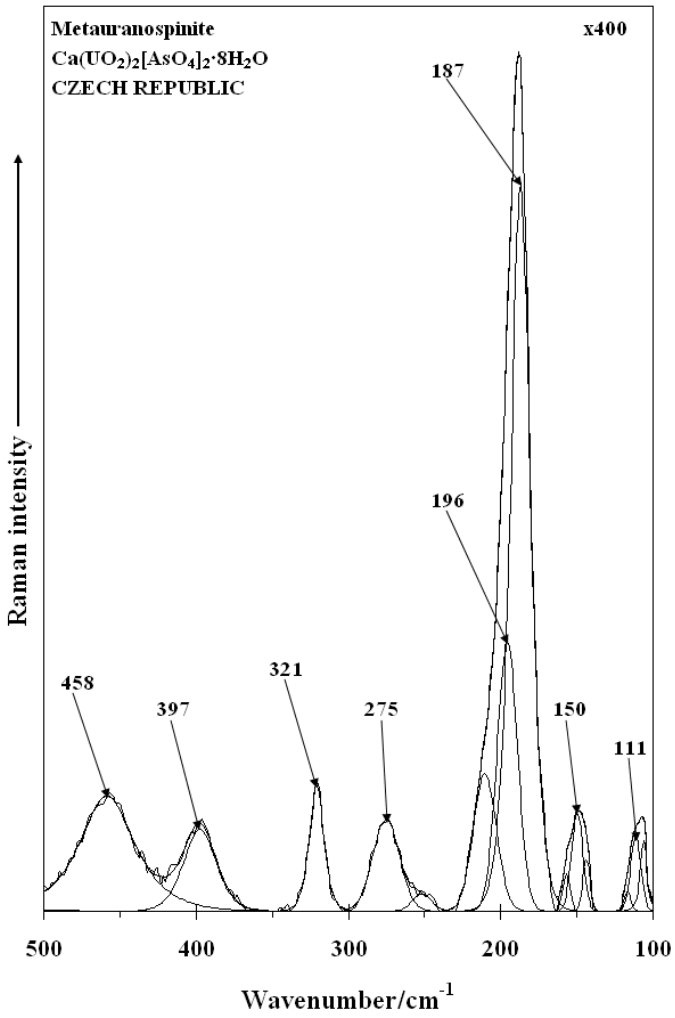

359

360

361 **Figure 2**

362

363

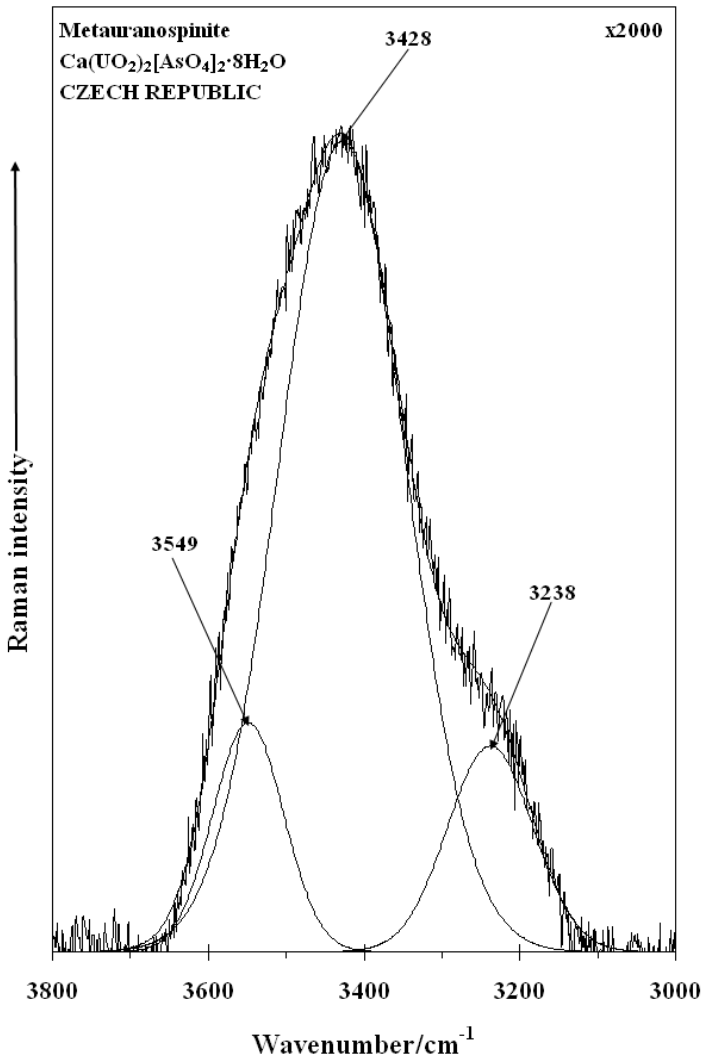

364

365

366 **Figure 3**

367

368

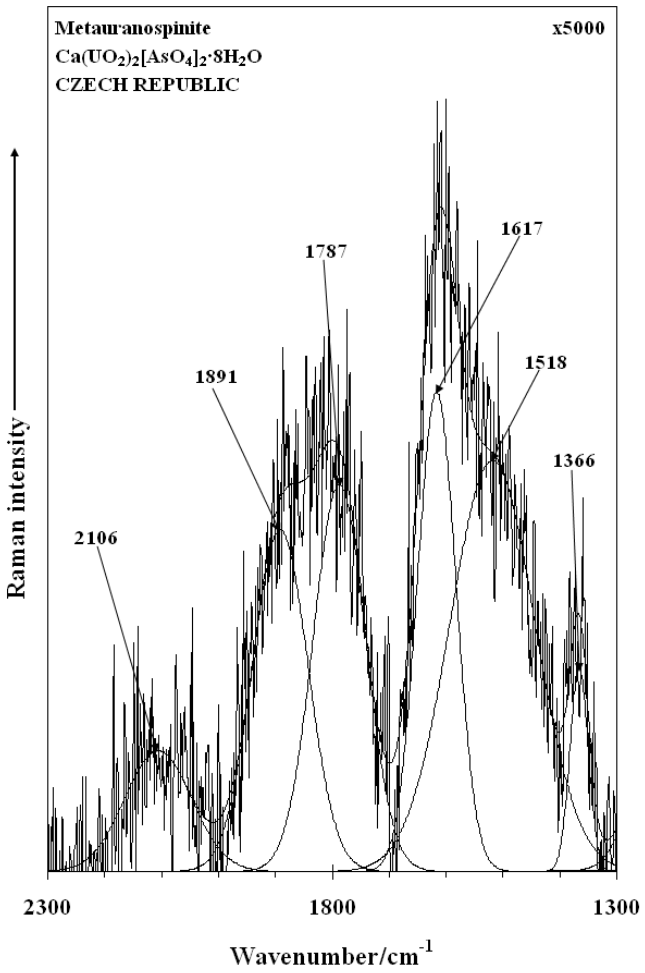

369

370

371 **Figure 4**

372

373

374